

# Centrality Dependence of Charm Production from Single Electrons Measurement in Au+Au Collisions at $\sqrt{s_{NN}} = 200$ GeV

S.S. Adler,<sup>5</sup> S. Afanasiev,<sup>17</sup> C. Aidala,<sup>5</sup> N.N. Ajitanand,<sup>43</sup> Y. Akiba,<sup>20,38</sup> J. Alexander,<sup>43</sup> R. Amirkas,<sup>12</sup> L. Aphecetche,<sup>45</sup> S.H. Aronson,<sup>5</sup> R. Auerbeck,<sup>44</sup> T.C. Awes,<sup>35</sup> R. Azmoun,<sup>44</sup> V. Babintsev,<sup>15</sup> A. Baldisseri,<sup>10</sup> K.N. Barish,<sup>6</sup> P.D. Barnes,<sup>27</sup> B. Bassalleck,<sup>33</sup> S. Bathe,<sup>30</sup> S. Batsouli,<sup>9</sup> V. Baublis,<sup>37</sup> A. Bazilevsky,<sup>39,15</sup> S. Belikov,<sup>16,15</sup> Y. Berdnikov,<sup>40</sup> S. Bhagavatula,<sup>16</sup> J.G. Boissevain,<sup>27</sup> H. Borel,<sup>10</sup> S. Borenstein,<sup>25</sup> M.L. Brooks,<sup>27</sup> D.S. Brown,<sup>34</sup> N. Bruner,<sup>33</sup> D. Bucher,<sup>30</sup> H. Buesching,<sup>30</sup> V. Bumazhnov,<sup>15</sup> G. Bunce,<sup>5,39</sup> J.M. Burward-Hoy,<sup>26,44</sup> S. Butsyk,<sup>44</sup> X. Camard,<sup>45</sup> J.-S. Chai,<sup>18</sup> P. Chand,<sup>4</sup> W.C. Chang,<sup>2</sup> S. Chernichenko,<sup>15</sup> C.Y. Chi,<sup>9</sup> J. Chiba,<sup>20</sup> M. Chiu,<sup>9</sup> I.J. Choi,<sup>52</sup> J. Choi,<sup>19</sup> R.K. Choudhury,<sup>4</sup> T. Chujo,<sup>5</sup> V. Cianciolo,<sup>35</sup> Y. Cobigo,<sup>10</sup> B.A. Cole,<sup>9</sup> P. Constantin,<sup>16</sup> D.G. d'Enterria,<sup>45</sup> G. David,<sup>5</sup> H. Delagrange,<sup>45</sup> A. Denisov,<sup>15</sup> A. Deshpande,<sup>39</sup> E.J. Desmond,<sup>5</sup> O. Dietzsch,<sup>41</sup> O. Drapier,<sup>25</sup> A. Drees,<sup>44</sup> R. du Rietz,<sup>29</sup> A. Durum,<sup>15</sup> D. Dutta,<sup>4</sup> Y.V. Efremenko,<sup>35</sup> K. El Chenawi,<sup>49</sup> A. Enokizono,<sup>14</sup> H. En'yo,<sup>38,39</sup> S. Esumi,<sup>48</sup> L. Ewell,<sup>5</sup> D.E. Fields,<sup>33,39</sup> F. Fleuret,<sup>25</sup> S.L. Fokin,<sup>23</sup> B.D. Fox,<sup>39</sup> Z. Fraenkel,<sup>51</sup> J.E. Frantz,<sup>9</sup> A. Franz,<sup>5</sup> A.D. Frawley,<sup>12</sup> S.-Y. Fung,<sup>6</sup> S. Garpman,<sup>29</sup> \* T.K. Ghosh,<sup>49</sup> A. Glenn,<sup>46</sup> G. Gogiberidze,<sup>46</sup> M. Gonin,<sup>25</sup> J. Gosset,<sup>10</sup> Y. Goto,<sup>39</sup> R. Granier de Cassagnac,<sup>25</sup> N. Grau,<sup>16</sup> S.V. Greene,<sup>49</sup> M. Grosse Perdekamp,<sup>39</sup> W. Guryn,<sup>5</sup> H.-Å. Gustafsson,<sup>29</sup> T. Hachiya,<sup>14</sup> J.S. Haggerty,<sup>5</sup> H. Hamagaki,<sup>8</sup> A.G. Hansen,<sup>27</sup> E.P. Hartouni,<sup>26</sup> M. Harvey,<sup>5</sup> R. Hayano,<sup>8</sup> X. He,<sup>13</sup> M. Heffner,<sup>26</sup> T.K. Hemmick,<sup>44</sup> J.M. Heuser,<sup>44</sup> M. Hibino,<sup>50</sup> J.C. Hill,<sup>16</sup> W. Holzmann,<sup>43</sup> K. Homma,<sup>14</sup> B. Hong,<sup>22</sup> A. Hoover,<sup>34</sup> T. Ichihara,<sup>38,39</sup> V.V. Ikonnikov,<sup>23</sup> K. Imai,<sup>24,38</sup> D. Isenhower,<sup>1</sup> M. Ishihara,<sup>38</sup> M. Issah,<sup>43</sup> A. Isupov,<sup>17</sup> B.V. Jacak,<sup>44</sup> W.Y. Jang,<sup>22</sup> Y. Jeong,<sup>19</sup> J. Jia,<sup>44</sup> O. Jinnouchi,<sup>38</sup> B.M. Johnson,<sup>5</sup> S.C. Johnson,<sup>26</sup> K.S. Joo,<sup>31</sup> D. Jouan,<sup>36</sup> S. Kametani,<sup>8,50</sup> N. Kamihara,<sup>47,38</sup> J.H. Kang,<sup>52</sup> S.S. Kapoor,<sup>4</sup> K. Katou,<sup>50</sup> S. Kelly,<sup>9</sup> B. Khachaturov,<sup>51</sup> A. Khanzadeev,<sup>37</sup> J. Kikuchi,<sup>50</sup> D.H. Kim,<sup>31</sup> D.J. Kim,<sup>52</sup> D.W. Kim,<sup>19</sup> E. Kim,<sup>42</sup> G.-B. Kim,<sup>25</sup> H.J. Kim,<sup>52</sup> E. Kistenev,<sup>5</sup> A. Kiyomichi,<sup>48</sup> K. Kiyoyama,<sup>32</sup> C. Klein-Boesing,<sup>30</sup> H. Kobayashi,<sup>38,39</sup> L. Kochenda,<sup>37</sup> V. Kochetkov,<sup>15</sup> D. Koehler,<sup>33</sup> T. Kohama,<sup>14</sup> M. Kopytine,<sup>44</sup> D. Kotchetkov,<sup>6</sup> A. Kozlov,<sup>51</sup> P.J. Kroon,<sup>5</sup> C.H. Kuberg,<sup>1,27</sup> K. Kurita,<sup>39</sup> Y. Kuroki,<sup>48</sup> M.J. Kweon,<sup>22</sup> Y. Kwon,<sup>52</sup> G.S. Kyle,<sup>34</sup> R. Lacey,<sup>43</sup> V. Ladygin,<sup>17</sup> J.G. Lajoie,<sup>16</sup> A. Lebedev,<sup>16,23</sup> S. Leckey,<sup>44</sup> D.M. Lee,<sup>27</sup> S. Lee,<sup>19</sup> M.J. Leitch,<sup>27</sup> X.H. Li,<sup>6</sup> H. Lim,<sup>42</sup> A. Litvinenko,<sup>17</sup> M.X. Liu,<sup>27</sup> Y. Liu,<sup>36</sup> C.F. Maguire,<sup>49</sup> Y.I. Makdisi,<sup>5</sup> A. Malakhov,<sup>17</sup> V.I. Manko,<sup>23</sup> Y. Mao,<sup>7,38</sup> G. Martinez,<sup>45</sup> M.D. Marx,<sup>44</sup> H. Masui,<sup>48</sup> F. Matathias,<sup>44</sup> T. Matsumoto,<sup>8,50</sup> P.L. McGaughey,<sup>27</sup> E. Melnikov,<sup>15</sup> F. Messer,<sup>44</sup> Y. Miake,<sup>48</sup> J. Milan,<sup>43</sup> T.E. Miller,<sup>49</sup> A. Milov,<sup>44,51</sup> S. Mioduszewski,<sup>5</sup> R.E. Mischke,<sup>27</sup> G.C. Mishra,<sup>13</sup> J.T. Mitchell,<sup>5</sup> A.K. Mohanty,<sup>4</sup> D.P. Morrison,<sup>5</sup> J.M. Moss,<sup>27</sup> F. Mühlbacher,<sup>44</sup> D. Mukhopadhyay,<sup>51</sup> M. Muniruzzaman,<sup>6</sup> J. Murata,<sup>38,39</sup> S. Nagamiya,<sup>20</sup> J.L. Nagle,<sup>9</sup> T. Nakamura,<sup>14</sup> B.K. Nandi,<sup>6</sup> M. Nara,<sup>48</sup> J. Newby,<sup>46</sup> P. Nilsson,<sup>29</sup> A.S. Nyanin,<sup>23</sup> J. Nystrand,<sup>29</sup> E. O'Brien,<sup>5</sup> C.A. Ogilvie,<sup>16</sup> H. Ohnishi,<sup>5,38</sup> I.D. Ojha,<sup>49,3</sup> K. Okada,<sup>38</sup> M. Ono,<sup>48</sup> V. Onuchin,<sup>15</sup> A. Oskarsson,<sup>29</sup> I. Otterlund,<sup>29</sup> K. Oyama,<sup>8</sup> K. Ozawa,<sup>8</sup> D. Pal,<sup>51</sup> A.P.T. Palounek,<sup>27</sup> V.S. Pantuev,<sup>44</sup> V. Papavassiliou,<sup>34</sup> J. Park,<sup>42</sup> A. Parmar,<sup>33</sup> S.F. Pate,<sup>34</sup> T. Peitzmann,<sup>30</sup> J.-C. Peng,<sup>27</sup> V. Peresedov,<sup>17</sup> C. Pinkenburg,<sup>5</sup> R.P. Pisani,<sup>5</sup> F. Plasil,<sup>35</sup> M.L. Purschke,<sup>5</sup> A.K. Purwar,<sup>44</sup> J. Rak,<sup>16</sup> I. Ravinovich,<sup>51</sup> K.F. Read,<sup>35,46</sup> M. Reuter,<sup>44</sup> K. Reygers,<sup>30</sup> V. Riabov,<sup>37,40</sup> Y. Riabov,<sup>37</sup> G. Roche,<sup>28</sup> A. Romana,<sup>25</sup> M. Rosati,<sup>16</sup> P. Rosnet,<sup>28</sup> S.S. Ryu,<sup>52</sup> M.E. Sadler,<sup>1</sup> N. Saito,<sup>38,39</sup> T. Sakaguchi,<sup>8,50</sup> M. Sakai,<sup>32</sup> S. Sakai,<sup>48</sup> V. Samsonov,<sup>37</sup> L. Sanfratello,<sup>33</sup> R. Santo,<sup>30</sup> H.D. Sato,<sup>24,38</sup> S. Sato,<sup>5,48</sup> S. Sawada,<sup>20</sup> Y. Schutz,<sup>45</sup> V. Semenov,<sup>15</sup> R. Seto,<sup>6</sup> M.R. Shaw,<sup>1,27</sup> T.K. Shea,<sup>5</sup> T.-A. Shibata,<sup>47,38</sup> K. Shigaki,<sup>14,20</sup> T. Shiina,<sup>27</sup> C.L. Silva,<sup>41</sup> D. Silvermyr,<sup>27,29</sup> K.S. Sim,<sup>22</sup> C.P. Singh,<sup>3</sup> V. Singh,<sup>3</sup> M. Sivertz,<sup>5</sup> A. Soldatov,<sup>15</sup> R.A. Soltz,<sup>26</sup> W.E. Sondheim,<sup>27</sup> S.P. Sorensen,<sup>46</sup> I.V. Sourikova,<sup>5</sup> F. Staley,<sup>10</sup> P.W. Stankus,<sup>35</sup> E. Stenlund,<sup>29</sup> M. Stepanov,<sup>34</sup> A. Ster,<sup>21</sup> S.P. Stoll,<sup>5</sup> T. Sugitate,<sup>14</sup> J.P. Sullivan,<sup>27</sup> E.M. Takagui,<sup>41</sup> A. Taketani,<sup>38,39</sup> M. Tamai,<sup>50</sup> K.H. Tanaka,<sup>20</sup> Y. Tanaka,<sup>32</sup> K. Tanida,<sup>38</sup> M.J. Tannenbaum,<sup>5</sup> P. Tarján,<sup>11</sup> J.D. Tepe,<sup>1,27</sup> T.L. Thomas,<sup>33</sup> J. Tojo,<sup>24,38</sup> H. Torii,<sup>24,38</sup> R.S. Towell,<sup>1</sup> I. Tseruya,<sup>51</sup> H. Tsuruoka,<sup>48</sup> S.K. Tuli,<sup>3</sup> H. Tydesjö,<sup>29</sup> N. Tyurin,<sup>15</sup> H.W. van Hecke,<sup>27</sup> J. Velkovska,<sup>5,44</sup> M. Velkovsky,<sup>44</sup> L. Villatte,<sup>46</sup> A.A. Vinogradov,<sup>23</sup> M.A. Volkov,<sup>23</sup> E. Vznuzdaev,<sup>37</sup> X.R. Wang,<sup>13</sup> Y. Watanabe,<sup>38,39</sup> S.N. White,<sup>5</sup> F.K. Wohn,<sup>16</sup> C.L. Woody,<sup>5</sup> W. Xie,<sup>6</sup> Y. Yang,<sup>7</sup> A. Yanovich,<sup>15</sup> S. Yokkaichi,<sup>38,39</sup> G.R. Young,<sup>35</sup> I.E. Yushmanov,<sup>23</sup> W.A. Zajc,<sup>9,†</sup> C. Zhang,<sup>9</sup> S. Zhou,<sup>7</sup> S.J. Zhou,<sup>51</sup> and L. Zolin<sup>17</sup>

(PHENIX Collaboration)

<sup>1</sup>Abilene Christian University, Abilene, TX 79699, USA

<sup>2</sup>Institute of Physics, Academia Sinica, Taipei 11529, Taiwan

<sup>3</sup>Department of Physics, Banaras Hindu University, Varanasi 221005, India

<sup>4</sup>Bhabha Atomic Research Centre, Bombay 400 085, India

- <sup>5</sup>Brookhaven National Laboratory, Upton, NY 11973-5000, USA  
<sup>6</sup>University of California - Riverside, Riverside, CA 92521, USA  
<sup>7</sup>China Institute of Atomic Energy (CIAE), Beijing, People's Republic of China  
<sup>8</sup>Center for Nuclear Study, Graduate School of Science, University of Tokyo, 7-3-1 Hongo, Bunkyo, Tokyo 113-0033, Japan  
<sup>9</sup>Columbia University, New York, NY 10027 and Nevis Laboratories, Irvington, NY 10533, USA  
<sup>10</sup>Dapnia, CEA Saclay, F-91191, Gif-sur-Yvette, France  
<sup>11</sup>Debrecen University, H-4010 Debrecen, Egyetem tér 1, Hungary  
<sup>12</sup>Florida State University, Tallahassee, FL 32306, USA  
<sup>13</sup>Georgia State University, Atlanta, GA 30303, USA  
<sup>14</sup>Hiroshima University, Kagamiyama, Higashi-Hiroshima 739-8526, Japan  
<sup>15</sup>Institute for High Energy Physics (IHEP), Protvino, Russia  
<sup>16</sup>Iowa State University, Ames, IA 50011, USA  
<sup>17</sup>Joint Institute for Nuclear Research, 141980 Dubna, Moscow Region, Russia  
<sup>18</sup>KAERI, Cyclotron Application Laboratory, Seoul, South Korea  
<sup>19</sup>Kangnung National University, Kangnung 210-702, South Korea  
<sup>20</sup>KEK, High Energy Accelerator Research Organization, Tsukuba-shi, Ibaraki-ken 305-0801, Japan  
<sup>21</sup>KFKI Research Institute for Particle and Nuclear Physics (RMKI), H-1525 Budapest 114, POBox 49, Hungary  
<sup>22</sup>Korea University, Seoul, 136-701, Korea  
<sup>23</sup>Russian Research Center "Kurchatov Institute", Moscow, Russia  
<sup>24</sup>Kyoto University, Kyoto 606, Japan  
<sup>25</sup>Laboratoire Leprince-Ringuet, Ecole Polytechnique, CNRS-IN2P3, Route de Saclay, F-91128, Palaiseau, France  
<sup>26</sup>Lawrence Livermore National Laboratory, Livermore, CA 94550, USA  
<sup>27</sup>Los Alamos National Laboratory, Los Alamos, NM 87545, USA  
<sup>28</sup>LPC, Université Blaise Pascal, CNRS-IN2P3, Clermont-Fd, 63177 Aubiere Cedex, France  
<sup>29</sup>Department of Physics, Lund University, Box 118, SE-221 00 Lund, Sweden  
<sup>30</sup>Institut für Kernphysik, University of Muenster, D-48149 Muenster, Germany  
<sup>31</sup>Myongji University, Yongin, Kyonggido 449-728, Korea  
<sup>32</sup>Nagasaki Institute of Applied Science, Nagasaki-shi, Nagasaki 851-0193, Japan  
<sup>33</sup>University of New Mexico, Albuquerque, NM 87131, USA  
<sup>34</sup>New Mexico State University, Las Cruces, NM 88003, USA  
<sup>35</sup>Oak Ridge National Laboratory, Oak Ridge, TN 37831, USA  
<sup>36</sup>IPN-Orsay, Université Paris Sud, CNRS-IN2P3, BP1, F-91406, Orsay, France  
<sup>37</sup>PNPI, Petersburg Nuclear Physics Institute, Gatchina, Russia  
<sup>38</sup>RIKEN (The Institute of Physical and Chemical Research), Wako, Saitama 351-0198, JAPAN  
<sup>39</sup>RIKEN BNL Research Center, Brookhaven National Laboratory, Upton, NY 11973-5000, USA  
<sup>40</sup>St. Petersburg State Technical University, St. Petersburg, Russia  
<sup>41</sup>Universidade de São Paulo, Instituto de Física, Caixa Postal 66318, São Paulo CEP05315-970, Brazil  
<sup>42</sup>System Electronics Laboratory, Seoul National University, Seoul, South Korea  
<sup>43</sup>Chemistry Department, Stony Brook University, SUNY, Stony Brook, NY 11794-3400, USA  
<sup>44</sup>Department of Physics and Astronomy, Stony Brook University, SUNY, Stony Brook, NY 11794, USA  
<sup>45</sup>SUBATECH (Ecole des Mines de Nantes, CNRS-IN2P3, Université de Nantes) BP 20722 - 44307, Nantes, France  
<sup>46</sup>University of Tennessee, Knoxville, TN 37996, USA  
<sup>47</sup>Department of Physics, Tokyo Institute of Technology, Tokyo, 152-8551, Japan  
<sup>48</sup>Institute of Physics, University of Tsukuba, Tsukuba, Ibaraki 305, Japan  
<sup>49</sup>Vanderbilt University, Nashville, TN 37235, USA  
<sup>50</sup>Waseda University, Advanced Research Institute for Science and Engineering, 17 Kikui-cho, Shinjuku-ku, Tokyo 162-0044, Japan  
<sup>51</sup>Weizmann Institute, Rehovot 76100, Israel  
<sup>52</sup>Yonsei University, IPAP, Seoul 120-749, Korea

(Dated: September 23, 2018)

The PHENIX experiment has measured mid-rapidity transverse momentum spectra ( $0.4 < p_T < 4.0 \text{ GeV}/c$ ) of single electrons as a function of centrality in Au+Au collisions at  $\sqrt{s_{NN}} = 200 \text{ GeV}$ . Contributions to the raw spectra from photon conversions and Dalitz decays of light neutral mesons are measured by introducing a thin (1.7%  $X_0$ ) converter into the PHENIX acceptance and are statistically removed. The subtracted "non-photonic" electron spectra are primarily due to the semi-leptonic decays of hadrons containing heavy quarks (charm and bottom). For all centralities, charm production cross section is found to scale with the nuclear overlap function,  $T_{AA}$ . For minimum-bias collisions the charm cross section per binary collision is  $N_{c\bar{c}}/T_{AA} = 622 \pm 57 \text{ (stat.)} \pm 160 \text{ (sys.)} \mu\text{b}$ .

PACS numbers: 25.75.Dw

In central Au+Au collisions at  $\sqrt{s_{NN}} = 200 \text{ GeV}$   $\pi^0$ 's and charged hadrons are strongly suppressed at high

transverse momentum ( $p_T$ ) [1, 2, 3]. In contrast, a modest high- $p_T$  enhancement is observed in d+Au collisions at the same energy [4, 5]. This strongly suggests that the suppression observed in Au+Au collisions is caused by final-state effects (*e.g.*, parton energy loss in a dense medium produced in the reaction [6, 7]).

Heavy quarks (charm and bottom) are complementary probes of the hot and dense matter produced in high energy heavy ion collisions. Due to their large masses, charm and bottom cross sections are calculable via pQCD and their yield is sensitive to the initial gluon density [8]. It has been predicted that heavy quarks suffer less energy loss than light quarks while traversing partonic matter due to the “dead cone” effect [9, 10, 11]. This can be studied through systematic measurements of the  $p_T$  spectra of open heavy flavor. In addition, the open-charm yield is an important baseline for understanding  $J/\psi$  production which has been predicted to be either suppressed [12] or enhanced [13] in the presence of de-confined quarks and gluons.

The PHENIX experiment observed that inclusive single electrons in central and minimum-bias Au+Au collisions at  $\sqrt{s_{NN}} = 130$  GeV were produced in excess of purely “photonic” contributions (primarily due to  $\pi^0$  Dalitz decays and conversion of  $\pi^0$  photons in the detector material) [14]. This excess is consistent with the expected charm production, assuming that it scales with the number of binary nucleon-nucleon collisions ( $N_{coll}$ ), or equivalently, with the nuclear overlap function,  $T_{AA}$ . In this Letter, we present results on the single electron measurement in  $\sqrt{s_{NN}} = 200$  GeV Au+Au collisions. The new data have higher statistics and smaller systematic errors than the 130 GeV data, allowing us to measure charm production as a function of collision centrality.

The data used in this analysis were collected by the PHENIX experiment [15] during the 2001 run period of the Relativistic Heavy Ion Collider. A coincidence of the beam-beam counters (BBC) and the zero degree calorimeters (ZDC) provides the minimum-bias trigger ( $92.2^{+2.5}_{-3.0}$  % of the  $6.8 \pm 0.5$  barn Au+Au inelastic cross section). The centrality is determined by the correlation between the multiplicity measured by the BBC and the energy of spectator neutrons measured by the ZDC. The BBC also measures the collision vertex,  $z$ , with resolution  $\sigma = 0.7$  cm. Events are required to have  $|z| < 20$  cm to eliminate electrons originating from the central magnet.

Charged particles are measured by the PHENIX east-arm spectrometer ( $|\eta| < 0.35$ ,  $\Delta\phi = \pi/4$ ) with resolution  $\sigma_p/p \simeq 0.7\% \oplus 1.0\% p(\text{GeV}/c)$ . Tracks are reconstructed with the drift chamber (DC) and the first layer of pad chambers (PC1) and confirmed by requiring an electromagnetic calorimeter (EMC) [16] matching hit within 2 standard deviations in position. Electron candidates are required to have at least three associated hits in the ring imaging Čerenkov detector (RICH) that pass a ring shape cut, and are required to pass a timing cut

in either the EMC or the time-of-flight detector. After these cuts, a clear electron signal is observed as a narrow peak at  $E/p = 1$ . By requiring  $-2\sigma < (E - p)/p < 3\sigma$ , background from hadrons, which deposit only a fraction of their energy in the EMC, and non-vertex electrons, which have mis-reconstructed momenta, is further reduced. Remaining background in the electron sample, due to accidental coincidences between RICH hits and hadron tracks, is estimated ( $\approx 10\%$ ) and subtracted by an event-mixing method.

Inclusive electrons contain two components: (1) “non-photonic” – primarily semi-leptonic decays of mesons containing heavy (charm and bottom) quarks, and (2) “photonic” – Dalitz decays of light neutral mesons ( $\pi^0$ ,  $\eta$ ,  $\eta'$ ,  $\rho$ ,  $\omega$  and  $\phi$ ) and photon conversions in the detector material. To separate these two components, a photon converter (a thin brass tube of 1.7% radiation length surrounding the beam pipe at  $r = 29$  cm) was installed.

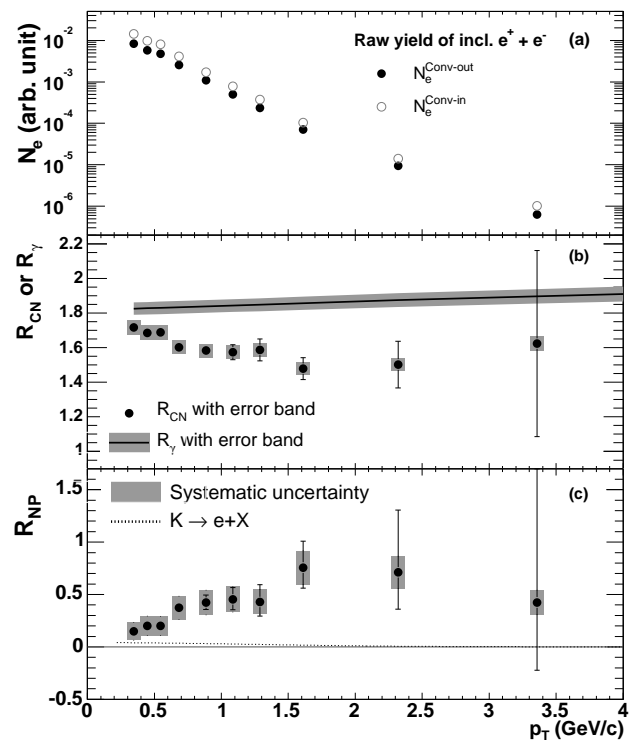


FIG. 1: Shown vs  $p_T$  (a) Raw  $e^\pm$  spectra measured with the converter in (open circles) and out (closed circles). (b) Ratio of the converter in/out  $e^\pm$  yields ( $R_{CN}$ , points) and ratio of photonic  $e^\pm$  yield with/without the converter ( $R_\gamma$ , line and shaded band). (c) Ratio of non-photonic to photonic  $e^\pm$  yields ( $R_{NP}$ , points) and contribution from kaon decays (dashed line).

We analyzed 2.2 M (2.5 M) events with the converter in (out). The corresponding raw electron  $p_T$  spectra for minimum-bias collisions are shown in Fig. 1(a). The photon converter multiplies the photonic contribution to the

electron yield by a factor  $R_\gamma$ :

$$N_e^{Conv-out} = N_e^\gamma + N_e^{non-\gamma} \quad (1)$$

$$N_e^{Conv-in} = R_\gamma N_e^\gamma + (1 - \epsilon) \cdot N_e^{non-\gamma} \quad (2)$$

Here  $N_e^{Conv-in}$  ( $N_e^{Conv-out}$ ) is the measured electron yield with (without) the converter;  $N_e^\gamma$  ( $N_e^{non-\gamma}$ ) is the electron yield due to the photonic (non-photonic) component; and  $\epsilon$  ( $\approx 2.1\%$ ) represents a small loss of electrons due to the converter. We next define  $R_{CN}$  as the ratio of the raw electron yield with and without the converter. Dividing Eq. (2) by Eq. (1) and defining  $R_{NP} \equiv N_e^{non-\gamma}/N_e^\gamma$ , one has:

$$R_{CN} \equiv \frac{N_e^{Conv-in}}{N_e^{Conv-out}} = \frac{R_\gamma + (1 - \epsilon)R_{NP}}{1 + R_{NP}} \quad (3)$$

If there were no contribution from non-photonic component ( $R_{NP} = 0$ ), then  $R_{CN} = R_\gamma$ .

The photonic electron yield per photon is approximately given by  $Y \propto \delta + \frac{7}{9}t$ , where  $\delta$  is the Dalitz branching ratio per  $\gamma$  relative to  $2\gamma$  (for  $\pi^0, \eta, \eta'$ ) or  $1\gamma$  (for  $\rho, \omega$  and  $\phi$ ) decay, and  $t$  is the thickness of the conversion material in radiation length ( $X_0$ ). The factor  $\frac{7}{9}$  is the approximate probability for a  $\gamma$  to convert in one  $X_0$ . Plugging in  $\delta^{\pi^0} = 0.6\%$ ,  $t \approx 1.1\%$  ( $t \approx 2.8\%$ ) for converter in (out) we find  $R_\gamma^{\pi^0} = Y^{Conv-in}/Y^{Conv-out} \approx 1.9$ . There is some  $p_T$  dependence in the complete formula for  $Y$  and the value of  $\delta$  is species-dependent ( $\delta^\eta \approx 0.8\%$ ), so we perform a full GEANT [17] simulation with and without the converter to calculate  $R_\gamma$ . We determine  $R_\gamma$  for  $\pi^0$  and  $\eta$  separately. We use the  $\pi^0$  spectrum measured by PHENIX [1] as the input for the  $\pi^0$  simulation and assume  $m_T$  scaling ( $p_T \rightarrow \sqrt{p_T^2 + M_\eta^2} - M_\pi^2$ , normalized at high  $p_T$  to  $\eta/\pi^0 = 0.45 \pm 0.1$ , based on the world data of  $\eta/\pi^0$  ratio) to obtain the input for the  $\eta$  simulation. Contributions from other mesons which undergo Dalitz decay ( $\eta', \rho, \omega, \phi$ ) are small (6% at  $p_T = 3 \text{ GeV}/c$ , and smaller at lower  $p_T$ ). Since they have  $\delta \approx \delta^\eta$  we assign them  $R_\gamma = R_\gamma^\eta$ . When calculating the combined  $R_\gamma$  we use the particle ratios at high  $p_T$  ( $\eta'/\pi^0 = 0.25 \pm 0.13$ ,  $\rho/\pi^0 = \omega/\pi^0 = 1 \pm 0.5$ ,  $\phi/\pi^0 = 0.4 \pm 0.2$ ). The  $\phi/\pi^0$  ratio used here is consistent with our  $\pi^0$  and  $\phi$  measurement [18]. The uncertainties in the particle ratios are included in the systematic uncertainties of  $R_\gamma$ . For this method it is essential that the amount of material is accurately modeled in the simulation. We compared the yield of identified photon conversion pairs in the data and in the simulation and conclude that the simulation reproduces  $R_\gamma$  within  $\pm 2.0\%$ . This uncertainty is included in the overall systematic uncertainty.

Fig. 1(b) shows  $R_{CN}$  and  $R_\gamma$  vs.  $p_T$ .  $R_{CN}$  gradually decreases with increasing  $p_T$ , while  $R_\gamma$  slightly increases with  $p_T$ . The difference between  $R_{CN}$  and  $R_\gamma$  indicates the existence of non-photonic electrons. Fig. 1(c) shows  $R_{NP}$  obtained from  $R_\gamma$  and  $R_{CN}$  using Eq. (3).  $R_{NP}$  increases with  $p_T$  and is more than 30% for  $p_T >$

0.6 GeV/ $c$ . The small amount of conversion material in the PHENIX detector allows a sensitive measurement of  $R_{CN}$ .

Background from kaon decays ( $K \rightarrow \pi e \nu$ ) and di-electron decays of  $\rho, \omega$  and  $\phi$  remain in the non-photonic electron yield. The background from kaon decays is estimated with a GEANT simulation using the kaon  $p_T$  spectrum measured by PHENIX [19] as input. The contribution of kaon decays to the non-photonic yield, shown in Fig. 1(c), is 18% at  $p_T = 0.4 \text{ GeV}/c$  and decreases rapidly to less than 6% for  $p_T > 1 \text{ GeV}/c$ .

To calculate background from the  $e^+e^-$  decays of  $\rho, \omega$  and  $\phi$ , we first generate spectra by applying  $m_T$  scaling to the PHENIX  $\pi^0$  spectrum, as described above. The contribution of these decays to the non-photonic electrons is  $< 3\%$  for all  $p_T$ . Background from  $J/\psi \rightarrow e^+e^-$  decays and from Drell-Yan pairs is negligible. Possible enhancement of low mass di-leptons through  $\pi + \pi \rightarrow \rho \rightarrow e^+e^-$ , as reported in Pb+Pb collisions at the SPS [20], would contribute to the non-photonic electrons. However, this is neglected since the estimated  $\rho$  contribution in the absence of enhancement is only  $\approx 0.6\%$  over all  $p_T$ .

After these backgrounds are subtracted the only other significant source of non-photonic electrons is the semi-leptonic decay of heavy flavor (charm and bottom). The raw spectrum of heavy flavor electrons is corrected for geometrical acceptance ( $\epsilon_{geo}$ ), track reconstruction efficiency ( $\epsilon_{rec}$ ) and electron identification efficiency ( $\epsilon_{eID}$ ) determined by GEANT simulation. The efficiency  $\epsilon_{geo} \times \epsilon_{rec}$  is about 11% of  $dN_e/dy$ , and  $\epsilon_{eID}$  is about 65% as confirmed with electrons identified through photon conversion. Correction of multiplicity dependent efficiency losses, estimated by embedding simulated electron tracks into real events, is  $p_T$ -independent and increases from 5% to 26% from peripheral to central collisions. The  $1\sigma$  systematic uncertainty of these corrections is 11.8%. Fully corrected heavy flavor electron spectra are shown in Fig. 2 for minimum-bias collisions and for five centrality bins.

PHENIX has also measured the heavy flavor electron spectrum in  $p+p$  collisions at  $\sqrt{s_{NN}} = 200 \text{ GeV}$  [21]. The lines in Fig. 2 show the best fit curve of this spectrum, scaled by  $T_{AA}$  for each Au+Au centrality bin. Here,  $T_{AA}$  is the nuclear overlap function calculated by a Glauber model [1](Table I). The Au+Au data points are in reasonable agreement with the  $p+p$  fit in all centrality bins.

To quantify the centrality dependence of heavy flavor production, we calculated the integrated yield  $dN_e/dy$  ( $0.8 < p_T < 4.0 \text{ GeV}/c$ ) and fit it to  $AN_{coll}^\alpha$ , where  $\alpha = 1$  is the expectation in the absence of medium effects. In this comparison, most of the systematic effects will cancel. Figure 3 shows  $dN_e/dy(0.8 < p_T < 4.0)/N_{coll}$  vs.  $N_{coll}$  for minimum-bias and five centrality bins in Au+Au collisions and  $p+p$  collisions. We find  $\alpha = 0.938 \pm 0.075(\text{stat.}) \pm 0.018(\text{sys.})$ . If  $p+p$  data is included,  $\alpha = 0.958 \pm 0.035(\text{stat.})$ . This shows that the

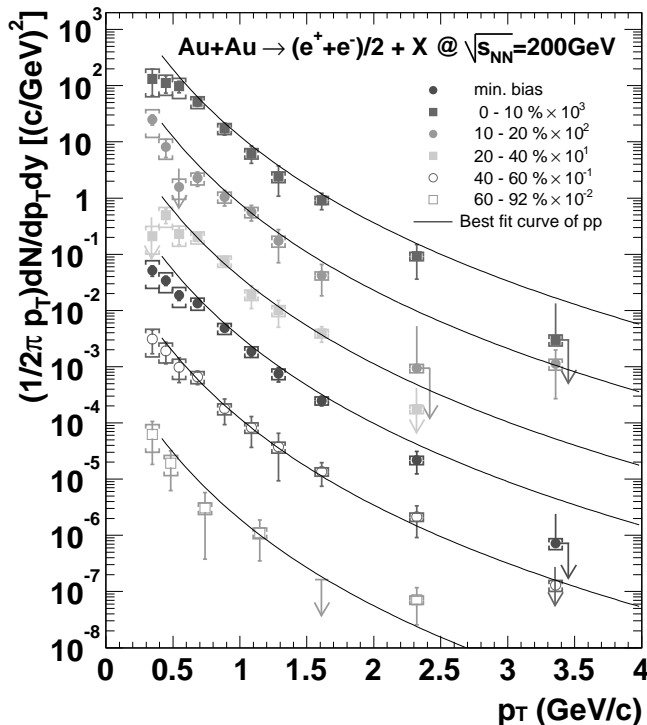


FIG. 2: Fully corrected heavy flavor electron  $p_T$  spectra for different Au+Au centralities scaled by successive factors of ten for clarity. Error bars (brackets) correspond to statistical (systematic) uncertainties. Curves are described in the text.

total yield of heavy flavor electrons for all centralities is consistent with  $N_{coll}$  scaling.

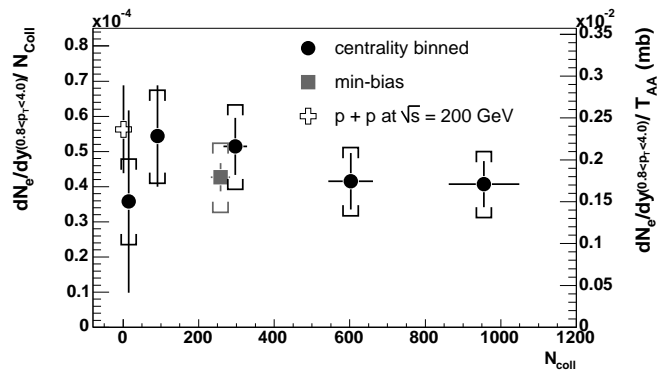


FIG. 3: Non-photonic electron yield ( $0.8 < p_T < 4.0$  GeV/c) measured in Au+Au reactions at 200 GeV scaled by  $N_{coll}$  (left-hand scale) as a function of centrality given by  $N_{coll}$ . This electron yield translates to the electron cross section per  $NN$  collision in the above  $p_T$  range (right-hand scale). The yield in  $p + p$  collisions at 200 GeV is also shown [21].

For each centrality bin we scale the heavy flavor electron spectrum ( $p_T > 0.8$  GeV/c) by  $T_{AA}$  and fit it with a PYTHIA calculation of the electron spectrum resulting from leading order charm and bottom production. We used PYTHIA 6.205 with a modified set of parameters

(described in [14]) and CTEQ5L PDFs [22]. Based on experimental input [23, 24] we modified the PYTHIA default charm ratios, using instead  $D^+/D^0 = 0.45 \pm 0.1$ ,  $D_s/D^0 = 0.25 \pm 0.1$ ,  $\Lambda_c/D^0 = 0.1 \pm 0.05$ . This gives a  $c$ -quark  $\rightarrow e$  total branching ratio of  $9.5 \pm 0.4\%$ . The scaled charm and bottom cross sections are treated as fit parameters, although we find that our data are restricted to  $p_T$  values which are only sensitive to charm production. We evaluated the systematic error due to background subtraction ( $\approx 21\%$ ) by refitting to the electron spectrum at the minimum and maximum of its  $1\sigma$  systematic error band. The change of the  $p_T$  range for fitting the non-photonic electron spectrum gives 3% systematic error for minimum-bias collisions. The systematic error due to the PYTHIA spectral shape ( $\approx 11\%$ ) is dominated by the uncertainty in  $\langle k_T \rangle = 1.5 \pm 0.5$  GeV/c. Different PDFs yield a systematic error of 6.2% for the rapidity-integrated cross section. Systematic errors in  $T_{AA}$  are tabulated in [1]. These systematic errors are added in quadrature to give the overall systematic error on the charm cross section. For minimum-bias collisions we obtain  $\frac{1}{T_{AA}} \frac{dN_{c\bar{c}}}{dy} |_{y=0} = 143 \pm 13(\text{stat.}) \pm 36(\text{sys.}) \mu\text{b}$  and  $N_{c\bar{c}}/T_{AA} = 622 \pm 57(\text{stat.}) \pm 160(\text{sys.}) \mu\text{b}$ . Results for all centrality bins are shown in Table I. The STAR collaboration reports somewhat larger charm cross section ( $1.3 \pm 0.2 \pm 0.4$  mb per  $NN$  collision) in  $p + p$  and  $d + \text{Au}$  collision at  $\sqrt{s_{NN}} = 200$  GeV [25]. The next-to-leading order pQCD calculation of charm cross section is 300 to 450  $\mu\text{b}$  [26].

TABLE I: Centrality bin, number of  $NN$  collisions, nuclear overlap function, charm cross section per  $NN$  collision, and total charm multiplicity per  $NN$  collision, in  $\sqrt{s_{NN}} = 200$  GeV Au+Au reactions.

Centrality	$N_{coll}$	$T_{AA}$ ( $\text{mb}^{-1}$ )	$\frac{1}{T_{AA}} \frac{dN_{c\bar{c}}}{dy}  _{y=0}$ ( $\mu\text{b}$ )	$N_{c\bar{c}}/T_{AA}$ ( $\mu\text{b}$ )
min. bias	$258 \pm 25$	$6.14 \pm 0.45$	$143 \pm 13 \pm 36$	$622 \pm 57 \pm 160$
0–10 %	$955 \pm 94$	$22.8 \pm 1.6$	$137 \pm 21 \pm 35$	$597 \pm 93 \pm 156$
10–20 %	$603 \pm 59$	$14.4 \pm 1.0$	$137 \pm 26 \pm 35$	$596 \pm 115 \pm 158$
20–40 %	$297 \pm 31$	$7.07 \pm 0.58$	$168 \pm 27 \pm 45$	$731 \pm 117 \pm 199$
40–60 %	$91 \pm 12$	$2.16 \pm 0.26$	$193 \pm 47 \pm 52$	$841 \pm 205 \pm 232$
60–92 %	$14.5 \pm 4.0$	$0.35 \pm 0.10$	$116 \pm 87 \pm 43$	$504 \pm 378 \pm 190$

It should be noted that final-state effects only influence the momentum distribution of charm; they have little or no effect on the total open charm yield. Therefore, our results indicate  $N_{coll}$  scaling of the initial charm production, as expected for point-like pQCD processes. pQCD calculations without charm quark energy loss and hydrodynamic calculations assuming complete thermalization of charm quarks predict very similar heavy flavor electron spectra for  $p_T < 2$  GeV/c [27]. Differentiating between these opposite physical pictures is only possible for  $p_T > 2.5$  GeV/c, where statistics of the current analysis

are limited.

In conclusion, we have measured single electrons from heavy flavor decays in Au + Au collisions at  $\sqrt{s_{NN}} = 200$  GeV. We observe that the centrality dependence of charm quark production is consistent with  $N_{coll}$  scaling, as expected for hard processes. The much larger Au + Au data set collected by PHENIX in the 2003-04 run will allow us more detailed exploration of medium effects on heavy quark production, both through deviations of the heavy flavor electron spectrum from  $N_{coll}$  scaling, and also through a measurement of charm quark flow.

We thank the staff of the Collider-Accelerator and Physics Departments at BNL for their vital contributions. We acknowledge support from the Department of Energy and NSF (U.S.A.), MEXT and JSPS (Japan), CNPq and FAPESP (Brazil), NSFC (China), CNRS-IN2P3 and CEA (France), BMBF, DAAD, and AvH (Germany), OTKA (Hungary), DAE and DST (India), ISF (Israel), KRF and CHEP (Korea), RMIST, RAS, and RMAE, (Russia), VR and KAW (Sweden), U.S. CRDF for the FSU, US-Hungarian NSF-OTKA-MTA, and US-Israel BSF.

---

\* Deceased

† PHENIX Spokesperson:zajc@nevis.columbia.edu

- [1] S.S. Adler *et al.*, Phys. Rev. Lett. **91**, 072301 (2003).
- [2] J. Adams *et al.*, Phys. Rev. Lett. **91**, 172302 (2003).
- [3] S.S. Adler *et al.*, Phys. Rev. C**69**, 034910 (2004).
- [4] S.S. Adler *et al.*, Phys. Rev. Lett. **91**, 072303 (2003).

- [5] J. Adams *et al.*, Phys. Rev. Lett. **91**, 072304 (2003).
- [6] Munshi Golam Mustafa, Dipali Pal, Dinesh Kumar Srivastava, and Markus Thoma, Phys. Lett. B**428**, 234 (1998).
- [7] Z. Lin, R. Vogt, and X.N. Wang, Phys. Rev. C**57**, 899, (1998).
- [8] J.A. Appel, Ann. Rev. Nucl. Part. Sci. **42**, 367 (1992).
- [9] Y.L. Dokshitzer and D.E. Kharzeev, Phys. Lett. B**519**, 199 (2001).
- [10] M. Djordjevic and M. Gyulassy, Phys. Lett. B**560**, 37 (2003).
- [11] B.W. Zhang, E. Wang and X-N. Wang, Phys. Rev. Lett. **93**, 072301 (2004).
- [12] T. Matsui and H. Satz, Phys. Lett. B**178**, 416 (1986).
- [13] R.L. Thews, M. Schroedter and J. Rafelski, Phys. Rev. C**63**, 054905 (2001).
- [14] K. Adcox *et al.*, Phys. Rev. Lett. **88**, 192303 (2002).
- [15] K. Adcox *et al.*, Nucl. Instrum. Methods **A499**, 469 (2003).
- [16] L. Aphecetche *et al.*, Nucl. Instrum. Methods **A499**, 521 (2003).
- [17] GEANT 3.2.1, CERN program library.
- [18] R. Seto *et al.*, J. Phys **G30**, S1017 (2004)
- [19] S.S. Adler *et al.*, Phys. Rev. C **69**, 034909 (2004).
- [20] G. Agakichiev *et al.*, Phys. Lett. B**422**, 405 (1998).
- [21] S. Kelly *et al.*, J. Phys **G30**, S1189 (2004)
- [22] H.L. Lai *et al.*, Eur. Phys. J. **C12**, 375 (2000).
- [23] D. Acosta *et al.*, Phys. Rev. Lett. **91**, 241804 (2003).
- [24] Review of Particle Physics, Phys. Rev. D**66**, 010001 (2002)
- [25] J. Adams *et al.*, nucl-ex/0407006.
- [26] R. Vogt, hep-ph/0203151.
- [27] S. Batsouli *et al.*, Phys. Lett. B**557**, 26 (2003).